doi:10.1093/brain/awn018 *Brain* (2008), **131**, 945–961

Disrupted small-world networks in schizophrenia

Yong Liu,[1] Meng Liang,[1,2] Yuan Zhou,[1] Yong He,[1,3] Yihui Hao,[4] Ming Song,[1] Chunshui Yu,[5] Haihong Liu,[4] Zhening Liu[4] and Tianzi Jiang[1]

[1]National Laboratory of Pattern Recognition, Institute of Automation, Chinese Academy of Sciences, Beijing 100080, People's Republic of China, [2]Department of Physiology, Anatomy, and Genetics University of Oxford, Oxford OX1 3QX, UK, [3]McConnell Brain Imaging Centre, Montreal Neurological Institute, McGill University, Montreal, Quebec H3A 2B4, Canada, [4]Institute of Mental Health, Second Xiangya Hospital, Central South University, Changsha 410011, Hunan, China and [5]Department of Radiology, Xuanwu Hospital of Capital Medical University, Beijing 100053, People's Republic of China

Correspondence to: Tianzi Jiang, National Laboratory of Pattern Recognition, Institute of Automation, Chinese Academy of Sciences, Beijing 100080, China
E-mail: jiangtz@nlpr.ia.ac.cn

The human brain has been described as a large, sparse, complex network characterized by efficient small-world properties, which assure that the brain generates and integrates information with high efficiency. Many previous neuroimaging studies have provided consistent evidence of 'dysfunctional connectivity' among the brain regions in schizophrenia; however, little is known about whether or not this dysfunctional connectivity causes disruption of the topological properties of brain functional networks. To this end, we investigated the topological properties of human brain functional networks derived from resting-state functional magnetic resonance imaging (fMRI). Data was obtained from 31 schizophrenia patients and 31 healthy subjects; then functional connectivity between 90 cortical and sub-cortical regions was estimated by partial correlation analysis and thresholded to construct a set of undirected graphs. Our findings demonstrated that the brain functional networks had efficient small-world properties in the healthy subjects; whereas these properties were disrupted in the patients with schizophrenia. Brain functional networks have efficient small-world properties which support efficient parallel information transfer at a relatively low cost. More importantly, in patients with schizophrenia the small-world topological properties are significantly altered in many brain regions in the prefrontal, parietal and temporal lobes. These findings are consistent with a hypothesis of dysfunctional integration of the brain in this illness. Specifically, we found that these altered topological measurements correlate with illness duration in schizophrenia. Detection and estimation of these alterations could prove helpful for understanding the pathophysiological mechanism as well as for evaluation of the severity of schizophrenia.

Keywords: efficient small-world; brain functional networks; functional connectivity; resting-state fMRI; schizophrenia

Abbreviations: BOLD = blood oxygenation level dependent; EPI = echo planar imaging; fMRI = functional magnetic resonance imaging; PANSS = Positive and Negative Syndrome Scale

Received September 14, 2007. Revised January 4, 2008. Accepted January 25, 2008. Advance Access publication February 25, 2008

Introduction

The human brain has evolved to support rapid real-time integration of information across segregated sensory brain regions (Sporns and Zwi, 2004), to confer resilience against pathological attack (Achard *et al.*, 2006), and to maximize efficiency at a minimal cost for effective information processing between different brain regions (Achard and Bullmore, 2007). Small-world networks offer a structural substrate for functional segregation and integration of the brain (Sporns and Zwi, 2004) and facilitate rapid adaptive reconfiguration of neuronal assemblies in support of changing cognitive states (Bassett and Bullmore, 2006). Efficiency provides a vital measure of how well information is transformed over a network (Achard and Bullmore, 2007). The combination of these factors makes efficient small-world topology an attractive model for brain functional networks.

In terms of the pathophysiology of schizophrenia, dysfunctional connectivity has been hypothesized to be the pathophysiological mechanism of cognitive dysfunction. Widely distributed dysfunctional connectivity, such as frontal-frontal/fronto-temporal disconnections (Friston and Frith, 1995; Andreasen *et al.*, 1998; Tan *et al.*, 2006), reduced connectivity between the fronto-parietal (Paulus *et al.*, 2002; Kim *et al.*, 2003), occipito-temporal (Kim *et al.*, 2005) and

dorsolateral prefrontal-anterior cingulate (Spence *et al.*, 2000) have been reported. Also disrupted interregional connectivity within the cortico-cerebellar-thalamo-cortical circuit (Honey *et al.*, 2005) and aberrant connectivity within default mode network (Bluhm *et al.*, 2007; Garrity *et al.*, 2007; Zhou *et al.*, 2007*b*) have been reported. The disruptions of interregional brain connectivity may lead to the failure of functional integration within the brain in schizophrenia. This failure may partially account for the deficits in cognition and behaviour of schizophrenia patients. So far, however, little is known about changes in the global/local structure of the brain functional network in schizophrenia except for the results of two recent studies using fMRI (Liang *et al.*, 2006*a*) and EEG data (Micheloyannis *et al.*, 2006*a*). Liang *et al.* (2006*a*) suggested altered small-world properties in schizophrenia based on resting-state fMRI data. However, a key problem with that study is that only two networks (one for each group) were constructed; thus the results were descriptive and no statistical conclusion was able to be drawn. Micheloyannis *et al.* (2006*a*) reported disrupted small-world properties of brain networks in different bands of EEG signals in schizophrenia. Although EEG supplies a high temporal resolution, it cannot reveal information about the exact activities of specific sub-cortical brain regions; thus EEGs cannot be used to construct a complete brain network.

To investigate directly the hypothesis that the brain network of schizophrenia is characterized by disruption of efficient small-world topological properties based on resting-state fMRI data, we divided the cerebrum into 90 brain regions. Functional connectivities were then estimated by calculating the partial correlation between the mean time series of each pair of brain regions for each subject. The resulting partial correlation matrices were thresholded to generate a set of undirected binary graphs. Topological parameters of brain networks were evaluated as a function of connectivity threshold, T, and the degree of connectivity, K. Statistical analyses were performed to explore the differences between patients and healthy subjects. Pearson's correlation coefficients between these topological properties and clinical variables were used to evaluate the relationship in schizophrenia.

Materials and Methods

Subjects

The study included 31 patients with schizophrenia (mean age of 24 years) who were recruited from the Institute of Mental Health, Second Xiangya Hospital, China. Confirmation of the diagnosis for all patients was made by clinical psychiatrists, using the Structured Clinical Interview for DSM-IV, Patient Version (First *et al.*, 1995). During the time of the experiments, trained and experienced psychiatrists assessed the symptoms of these patients using the Positive and Negative Syndrome Scale (PANSS). The mean treatment was 442 mg chlorpromazine-equivalent antipsychotic (21 subjects were receiving atypical antipsychotic medications and 10 were not receiving any medical treatment at the time of examination) (Table 1). Thirty-one age and gender-matched healthy subjects were recruited from similar geographic and demographic regions (Table 1).

Table 1 Demographic and clinical details of the subjects

	Controls ($n = 31$)	Schizophrenia ($n = 31$)	*P*-value
Gender (male)	16	17	0.8[a]
Age (years)	26 ± 4	24 ± 6	0.20[b]
Duration of illness (months)	–	27 ± 24	–
Medication dose (mg)	–	442 ± 208[c]	–
PANSS	–	83 ± 20	–

[a]The *P*-value was obtained by Pearson Chi-square.
[b]The *P*-value was obtained by two-sample two-tailed *t*-test.
[c]Chlorpromazine equivalent excluding 10 non-medications.

All subjects were right-handed. The exclusion criteria for all the subjects were as follows: no history of neurological or significant physical disorders, no history of alcohol or drug dependence and no history of receiving electroconvulsive therapy. All the healthy subjects had no history of psychiatric illness. Some of these subjects have been used in the previous studies (Liang *et al.*, 2006*a*, *b*; Zhou *et al.*, 2007*a*, *b*). All subjects gave voluntary and informed consent according to the standards set by the Ethics Committee of the Second Xiangya Hospital, Central South University.

Data acquisition and preprocessing

Imaging was performed on a 1.5 Tesla GE scanner in the Second Xiangya Hospital. Blood oxygenation level dependent (BOLD) images of the whole brain using an echo planar imaging (EPI) sequence were acquired in 20 axial slices (TR = 2000 ms, TE = 40 ms, flip angle = 90°, FOV = 24 cm; 5 mm thickness and 1 mm gap). The fMRI scanning was done in darkness. All the subjects were instructed to keep their eyes closed, not to think about anything in particular and to move as little as possible. For each subject, the fMRI scanning lasted 6 min. Structural sagittal images were obtained using a magnetization prepared rapid acquisition gradient echo three-dimensional T1-weighted sequence for each subject (TR = 2045 ms, TE = 9.6 ms, flip angle = 90°, FOV = 24 cm).

Unless specifically stated otherwise, all the preprocessing was carried out using statistical parametric mapping (SPM2, http://www.fil.ion.ucl.ac.uk/spm). To allow for magnetization equilibrium, the first 10 images were discarded. The remaining 170 images were first corrected for the acquisition time delay among different slices, and then the images were realigned to the first volume for head-motion correction. The time course of head motions was obtained by estimating the translations in each direction and the rotations in angular motion about each axis for each of the 170 consecutive volumes. All the subjects included in this study exhibited a maximum displacement of less than 1.5 mm at each axis and an angular motion of less than 1.5° for each axis. We also evaluated the group differences in translation and rotation of head motion according to the following formula:

$$\text{HeadMotion/Rotation} = \frac{1}{M-1}\sum_{i=2}^{M}\sqrt{|x_i - x_{i-1}|^2 + |y_i - y_{i-1}|^2 + |z_i - z_{i-1}|^2}$$

where M is the length of the time series ($M = 170$) in this study, x_i, y_i and z_i are translations/rotations at the ith time point in

Table 2 Cortical and sub-cortical regions defined in Automated Anatomical Labeling template image in standard stereotaxic space

Region name	Abbreviation	Region name	Abbreviation
Superior frontal gyrus, dorsolateral	SFGdor	Superior parietal gyrus	SPG
Superior frontal gyrus, orbital	SFGorb	Paracentral lobule	PCL
Superior frontal gyrus, medial	SFGmed	Postcentral gyrus	PoCG
Superior frontal gyrus, medial orbital	SFGmorb	Inferior parietal gyrus	IPG
Middle frontal gyrus	MFG	Supramarginal gyrus	SMG
Middle frontal gyrus, orbital	MFGorb	Angular gyrus	ANG
Inferior frontal gyrus, opercular	IFGoper	Precuneus	PCNU
Inferior frontal gyrus, triangular	IFGtri	Posterior cingulate gyrus	PCC
Inferior frontal gyrus, orbital	IFGorb		
Gyrus rectus	REG	Insula	INS
Anterior cingulate gyrus	ACC	Thalamus	THA
Olfactory cortex	OLF		
		Superior temporal gyrus	STG
Precentral gyrus	PreCG	Superior temporal gyrus, temporal pole	STGp
Supplementary motor area	SMA	Middle temporal gyrus	MTG
Rolandic operculum	ROL	Middle temporal gyrus, temporal pole	MTGp
Median- and para-cingulate gyrus	MCC	Inferior temporal gyrus	ITG
		Heschl gyrus	HES
Calcarine fissure and surrounding cortex	CAL	Hippocampus	HIP
Cuneus	CUN	Parahippocampal gyrus	PHIP
Lingual gyrus	LING	Amygdala	AMYG
Superior occipital gyrus	SOG		
Middle occipital gyrus	MOG	Caudate nucleus	CAU
Inferior occipital gyrus	IOG	Lenticular nucleus, putamen	PUT
Fusiform gyrus	FG	Lenticular nucleus, pallidum	PAL

the *x*, *y* and *z* directions, respectively (Liang *et al.*, 2006*b*). The results showed that the two groups had no significant differences in head motion (two sample two-tailed *t*-test, $P = 0.59$ for translational motion and $P = 0.55$ for rotational motion). The fMRI images were further spatially normalized to the Montreal Neurological Institute (MNI) EPI template and resampled to a 3 mm cubic voxel. Finally, temporal band-pass filtering ($0.01 < f < 0.08$ Hz) was performed in order to reduce the effects of low-frequency drift and high-frequency noise (Fox *et al.*, 2005; Liang *et al.*, 2006*b*; Liu *et al.*, 2007).

Anatomical parcellation

The registered fMRI data were segmented into 90 regions (45 for each hemisphere, Table 2) using the anatomically labelled template reported by Tzourio-Mazoyer *et al.* (2002), which has been used in several previous studies (Salvador *et al.*, 2005*a*, *b*; Achard *et al.*, 2006; Achard and Bullmore, 2007; Liang *et al.*, 2006*a*, *b*; Liu *et al.*, 2007). For each subject, the representative time series of each individual region was then obtained by simply averaging the fMRI time series over all voxels in this region. Each regional mean time-series was further corrected for the effect of head movement on the partial correlation coefficients by regression on the translations and rotations of the head estimated in the procedure of image realignment. The residuals of these regressions constituted the set of regional mean time-series used for undirected graph analysis (Salvador *et al.*, 2005*b*).

Estimation of the interregional partial correlations

Functional connectivity examines interregional correlations in neuronal variability (Friston *et al.*, 1993). Partial correlation can be used as a measure of the functional connectivity between a given pair of regions by attenuating the contribution of other sources of covariance (Whittaker, 1990; Hampson *et al.*, 2002). In this case, we used partial correlations to reduce indirect dependencies by other brain areas and built undirected graphs. Given a set of N random variables, the partial correlation matrix is a symmetric matrix in which each off-diagonal element is the correlation coefficient between a pair of variables after filtering out the contributions of all other variables included in the dataset. In the present study, therefore, the partial correlation between any pair of regions filters out the effects of the other 88 brain regions (Salvador *et al.*, 2005*a*).

The first step is to estimate the sample covariance matrix S from the data matrix $Y = (x_i)_{i=1,\ldots,90}$ of observations for each individual. Here x_i is the mean time series of each brain region. If we introduce $X = (x_j, x_k)$ to denote the average over time of the observations in the jth and kth regions, $Z = Y \backslash X$ denotes the other 88 mean time series matrices. Each component of S contains the sample covariance value between two regions (say j and k). If the covariance matrix of $[X, Z]$ is

$$S = \begin{pmatrix} S_{11} & S_{12} \\ S_{12}^T & S_{22} \end{pmatrix},$$

in which S_{11} is the covariance matrix of X, S_{12} is the covariance matrix of X and Z and S_{22} is the covariance matrix of Z, then the partial correlation matrix of X, controlling for Z, can be defined formally as a normalized version of the covariance matrix,

$$S_{xy} = S_{11} - S_{12} S_{22}^{-1} S_{12}^T.$$

Finally, a Fisher's *r*-to-*z* transformation is used on the partial correlation matrix in order to improve the normality of the partial correlation coefficients.

Graph theoretical analysis

Topological properties of the brain functional networks

An $N \times N$ ($N = 90$ in the present study) binary graph, G, consisting of nodes (brain regions) and undirected edges (functional connectivity) between nodes, can be constructed by applying a correlation threshold T (Fisher's r-to-z) to the partial correlation coefficients:

$$e_{ij} = \begin{cases} 1 & \text{if } |z(i,j)| \geq T \\ 0 & \text{otherwise} \end{cases}$$

That is, if the absolute $z(i, j)$ (Fisher r-to-z of the partial correlation coefficient) of a pair of brain regions, i and j, exceeds a given threshold T, an edge is said to exist; otherwise it does not exist. We define the subgraph G_i as the set of nodes that are the direct neighbours of the ith node, i.e. directly connected to the ith node with an edge. The degree of each node, $K_{i,i=1,2,\ldots,90}$, is defined as the number of nodes in the subgraph G_i. The degree of connectivity, K_p, of a graph is the average of the degrees of all the nodes in the graph:

$$K_p = \frac{1}{N}\sum_{i \in G} K_i,$$

which is a measure to evaluate the degree of sparsity of a network. The total number of edges in a graph, divided by the maximum possible number of edges $N(N-1)/2$:

$$K_{\text{cost}} = \frac{1}{N(N-1)}\sum_{i \in G} K_i,$$

is called the cost of the network, which measures how expensive it is to build the network (Latora and Marchiori, 2003). The connectivity strength of the ith node is:

$$E_{i\_\text{corr}} = \frac{1}{K_i}\sum_{j \in G_i} |z(i,j)| \cdot e_{ij}.$$

E_{i_corr} is a measure of the strength of the functional connectivity between the ith node and the nodes in the subgraph G_i. The strength of the functional connectivity of a graph is:

$$E_{\text{corr}} = \frac{1}{N}\sum_{i \in G} E_{i\_\text{corr}}.$$

The larger the E_{i_corr}, the stronger the functional connectivity of the brain functional network.

The absolute clustering coefficient of a node is the ratio of the number of existing connections to the number of all possible connections in the subgraph G_i:

$$C_i = \frac{E_i}{K_i(K_i-1)/2},$$

where E_i is the number of edges in the subgraph G_i (Watts and Strogatz, 1998; Strogatz, 2001). The absolute clustering coefficient of a network is the average of the absolute clustering coefficients of all nodes:

$$C_p = \frac{1}{N}\sum_{i \in G} C_i.$$

C_p is a measure of the extent of the local density or cliquishness of the network.

The mean shortest absolute path length of a node is:

$$L_i = \frac{1}{N-1}\sum_{i \neq j \in G} \min\{L_{i,j}\},$$

in which $\min\{L_{i,j}\}$ is the shortest absolute path length between the ith node and the jth node, and the absolute path length is the number of edges included in the path connecting two nodes. The mean shortest absolute path length of a network is the average of the shortest absolute path lengths between the nodes:

$$L_p = \frac{1}{N}\sum_{i \in G} L_i$$

L_p is a measure of the extent of average connectivity or overall routing efficiency of the network.

Compared with random networks, small-world networks have similar absolute path lengths but higher absolute clustering coefficients, that is $\gamma = C_p^{\text{real}}/C_p^{\text{rand}} > 1$, $\lambda = L_p^{\text{real}}/L_p^{\text{rand}} \approx 1$ (Watts and Strogatz, 1998). These two conditions can also be summarized into a scalar quantitative measurement, small-worldness, $\sigma = \gamma/\lambda$, which is typically >1 for small-world networks (Achard *et al.*, 2006; Humphries *et al.*, 2006; He *et al.*, 2007). To examine the small-world properties, the values of C_p^{real} and L_p^{real} of the functional brain network need to be compared with those of random networks. The theoretical values of these two measures for random networks are $C_p^{\text{rand}} = K/N$, and $L_p^{\text{rand}} \approx \ln(N)/\ln(K)$ (Achard *et al.*, 2006; Bassett and Bullmore, 2006; Stam *et al.*, 2007). However, as suggested by Stam *et al.* (2007), statistical comparisons should generally be performed between networks that have equal (or at least similar) degree sequences; however, theoretical random networks have Gaussian degree distributions that may differ from the degree distribution of the brain networks that we discovered in this study. To obtain a better control for the functional brain networks, we generated 100 random networks for each K and threshold T of each individual network by a Markov-chain algorithm (Maslov and Sneppen, 2002; Milo *et al.*, 2002; Sporns and Zwi, 2004). In the original matrix, if i_1 was connected to j_1 and i_2 was connected to j_2, for random matrices, we removed the edge between i_1 and j_1 but added an edge between i_1 and j_2. That means that a pair of vertices (i_1, j_1) and (i_2, j_2) was selected for which, $e_{i_1 j_1} = 1$, $e_{i_2 j_2} = 1$, $e_{i_1 j_2} = 0$, and $e_{i_2 j_1} = 0$. Then $e_{i_1 j_1} = 0$, $e_{i_2 j_2} = 1$, $e_{i_1 j_2} = 1$ and $e_{i_2 j_1} = 0$. Then we randomly permuted the matrix which assured that the random matrix had the same degree distribution as the original matrix. This procedure was repeated until the topological structure of the original matrix was randomized (Achard *et al.*, 2006). Then we averaged across all 100 generated random networks to obtain a mean C_p^{rand} and a mean L_p^{rand} for each degree K and threshold T.

Efficiency of small-world brain networks

It has been shown that brain functional networks have efficient small-world properties which support the efficient transfer of parallel information at a relatively low cost (Achard and Bullmore, 2007). E_{global}, a measure of the global efficiency of parallel information transfer in the network, is defined by the inverse of the harmonic mean of the minimum absolute path length between each pair of nodes (Latora and Marchiori, 2001, 2003; Achard and Bullmore, 2007):

$$E_{\text{global}} = \frac{1}{N(N-1)}\sum_{i \neq j \in G} \frac{1}{L_{i,j}}.$$

Table 3 Introduction of measurements and their meaning in the brain functional network

Character	Meaning
$z(i, j)$	z score of Fisher r-to-z transform of partial correlation coefficients
G_i	the set of nodes that are nearest neighbors of the ith node
K_p	degree of connectivity which evaluates the level of sparseness of a network
K_{cost}	cost of network
E_{corr}	mean z score of a brain functional network
C_p	clustering coefficient which measures the extent of a local cluster of the network
L_p	path length which measures of the extent of average connectivity of the network
γ	$\gamma = C_p^{real}/C_p^{rand}$, the ratio of the clustering coefficients between real and random network
λ	$\lambda = L_p^{real}/L_p^{rand}$ the ratio of the path length between real and random network
σ	$\sigma = \gamma/\lambda$, scalar quantitative measurement of the small-wordness of a network
E_{global}	a measure of the global efficiency of parallel information transfer in the network
E_{local}	a measure of the fault tolerance of the network

We can calculate the local efficiency of the ith node:

$$E_{i\_local} = \frac{1}{N_{G_i}(N_{G_i}-1)} \sum_{j,k \in G_i} \frac{1}{L_{j,k}}.$$

In fact, since the ith node is not an element of the subgraph G_i, the local efficiency can also be understood as a measure of the fault tolerance of the network, indicating how well each subgraph exchanges information when the index node is eliminated (Achard and Bullmore, 2007). In addition, based on its definition, it is a measure of the global efficiency of the subgraph G_i. The mean local efficiency of a graph, $E_{local} = (1/N)\sum_{i \in G} E_{i\_local}$, is the mean of all the local efficiencies of the nodes in the graph. We can also calculate the global efficiency (E_{global}) and local efficiency (E_{local}) as a function of K_{cost}.

Table 3 presents the measurements we have introduced and illustrates their meaning in human brain functional networks.

Statistical analysis

Statistical comparisons of E_{corr}, C_p^{real}, L_p^{real}, γ, λ, σ, E_{global} and E_{local} between the two groups were performed by using a two-sample two-tailed t-test for each value over a wide range of T or K (K_{cost}). For each selected threshold value, we also computed the mean degree of each subject and used a two-sample two-tailed t-test to determine if the degree of connectivity was significantly different between the two groups. If any change in the topological properties was found between the two groups, we investigated the distribution of the regions which showed significant differences in these topological properties.

Relationship between topological measures and clinical variables

We used Pearson's correlation coefficient to evaluate the relationship between the topological properties (E_{corr}, C_p^{real}, L_p^{real}, E_{global} and E_{local}) of the brain functional networks and various clinical variables (illness duration, PANSS scores and medication doses) for each T or K in the schizophrenia group. Because these analyses were exploratory in nature, we used a statistical significance level of $P < 0.05$ (uncorrected).

Results

Direct comparisons between schizophrenia and healthy subjects

The mean functional connectivity matrix of each group was calculated by averaging the $N \times N$ ($N = 90$ in the present study) absolute connection matrix of all the subjects within the group. In the normal group, most of the strong functional connectivities (large z-scores) were between inter-hemispheric homogenous regions, within a lobe, and between anatomically adjacent brain areas (Fig. 1). This functional connectivity pattern was consistent with many previous studies of whole brain functional connectivity in the resting-state (Salvador *et al.*, 2005a; Achard *et al.*, 2006). The schizophrenia group showed a similar functional connectivity pattern to that of the healthy group; however, the strength of the functional connectivity was lower in the schizophrenia group [$F(1,60) = 10.76$, $P = 0.002$].

Direct comparisons of all possible connections between the two groups were also performed to test the between-group differences. We found that the altered functional connectivities are distributed throughout the entire brain, which is consistent with a previous study by Liang *et al.* (2006*b*). Extended details about the methods and results can be found in part I of the supplemental material.

Efficient small-world properties of the two groups

Efficient small-world regime of brain functional networks

Following the studies by Stam and colleagues (2007), we investigated the topological properties of brain functional networks as a function of T or K (K_{cost}). Clearly the choice of a threshold value will have a major effect on the topological properties of the resulting networks: conservative thresholds, $T \to 1$, will generate sparsely connected graphs (with small K_p, more lenient thresholds, $T \to 0$, will generate more densely connected graphs (with large K_p, for $T = 0$, $K_p = 90$, $C_p^{real} = L_p^{real} = 1$), inevitably including a number of edges representing spurious or statistically non-significant correlations between regions. In the present study, we adopted the following complementary approaches to choose the thresholds:

(1) We thresholded all matrices using a single, conservative threshold chosen to construct a sparse graph with mean degree $K_p \geqslant 2\log N \approx 9$ (total number of edges $K \geqslant 405$). In addition, the maximum threshold (T) must also assure that each network is fully connected with $N = 90$ nodes. This allowed us to compare the

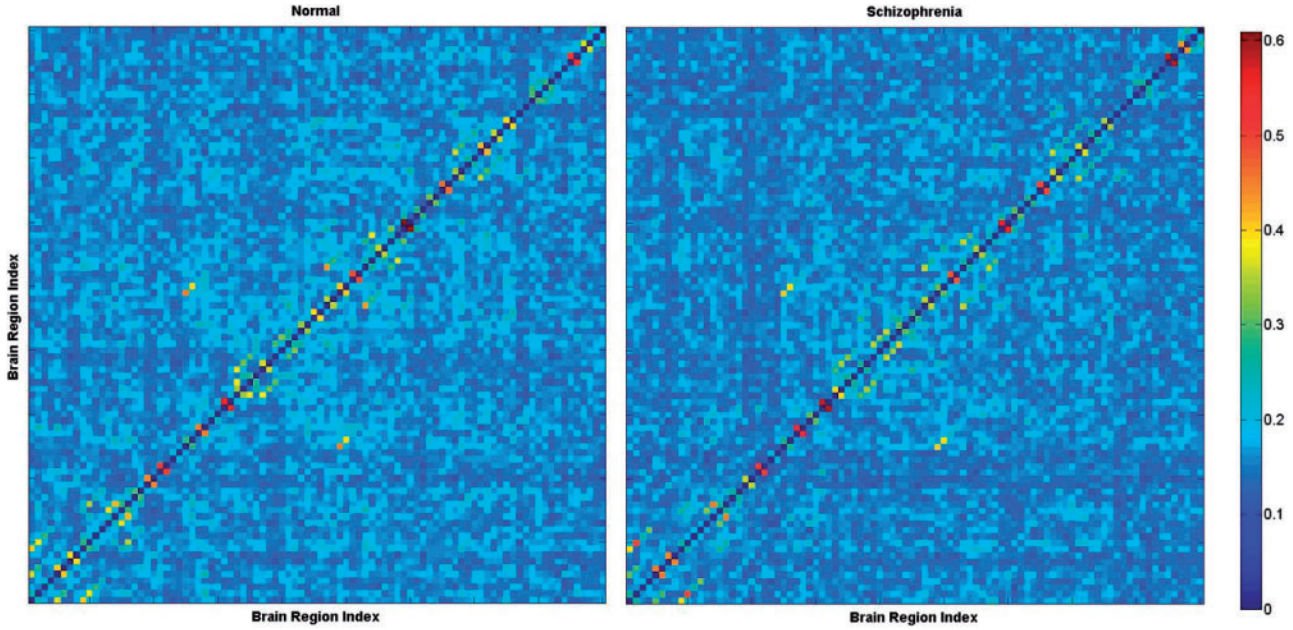

Fig. 1 Mean absolute *z*-score matrices for normal and schizophrenia group. Each figure shows a 90 × 90 square matrix, where the *x* and *y* axes correspond to the regions listed in Table 2, and where each entry indicates the mean strength of the functional connectivity between each pair of brain regions. The diagonal running from the lower left to the upper right is intentionally set to zero. The *z* score of the functional connectivity is indicated with a coloured bar.

topological properties between the two groups in a way that was relatively independent of the size of the network.

(2) The minimum threshold must ensure that the brain networks have a lower global efficiency and a larger local efficiency compared to random networks with relatively the same distribution of the degrees of connectivity, as suggested by Achard and Bullmore (2007).

We selected the threshold range, $T_{min} \leqslant T \leqslant T_{max}$ by intersecting the upper criteria. Then we repeated the full analysis for each value of T in the range $T_{min} \leqslant T \leqslant T_{max}$, with increments of 0.002. However, if the topological indices of the brain functional networks are only computed as a function of threshold T, the results could be influenced by differences in the number of edges between the two groups (Stam *et al.*, 2007). To control this effect, we repeated the analysis by computing the topological indices of each brain functional network as a function of the degree of connectivity, $K_{min} \leqslant K \leqslant K_{max}$ with steps of 0.22 (edge step/node = 20/90), where the range was determined in a manner similar to that described earlier. As shown in Fig. S5, brain networks were accepted as fully in both groups if the threshold $T \leqslant 0.316$ (Fig. S5); brain networks were accepted as fully connected if the total connected edge $\geqslant 490$ (that is $K_{cost} \geqslant (490/4005) \approx 0.122$) (Fig. S6). Consequently, we selected the small-world interval as $0.122 \leqslant K_{cost} \leqslant 0.267$ (the corresponding degree of connectivity threshold is $10.9 \leqslant K \leqslant 23.8$ and the corresponding connectivity threshold is $0.268 \leqslant T \leqslant 0.316$) (Fig. 2B). Such a range is similar to that used in Achard and Bullmore's study (2007).

Altered topological properties of brain functional networks in schizophrenia

The distributions of the degree of connectivity and the strength of the functional connectivity of the brain network as a function of threshold within each group are shown in Fig. 3. With an increase in the threshold, the degree of connectivity decreases; whereas the strength of the functional connectivity starts to increase because more and more edges with lower strength of the functional connectivities are being lost (providing a corresponding value of $z\text{-score} \leqslant T$). Over the whole range of threshold values (0.268–0.316), the degree (Fig. 3A) and strength of functional connectivity (Fig. 3B) were significantly lower in the schizophrenia group compared with the healthy group. The schizophrenia group also showed a significantly lower strength of functional connectivity than the healthy group over the whole range of K (Fig. 3C).

As shown in Fig. 4, the higher threshold resulted in a lower mean absolute clustering coefficient and a longer mean shortest absolute path length for both groups, as expected. Over the whole range of threshold values investigated (0.268–0.316), the absolute clustering coefficients of the healthy subjects were slightly higher than those of the schizophrenia group (Fig. 4A). For all values of T, the absolute path length was significantly longer in the schizophrenia group compared with the healthy

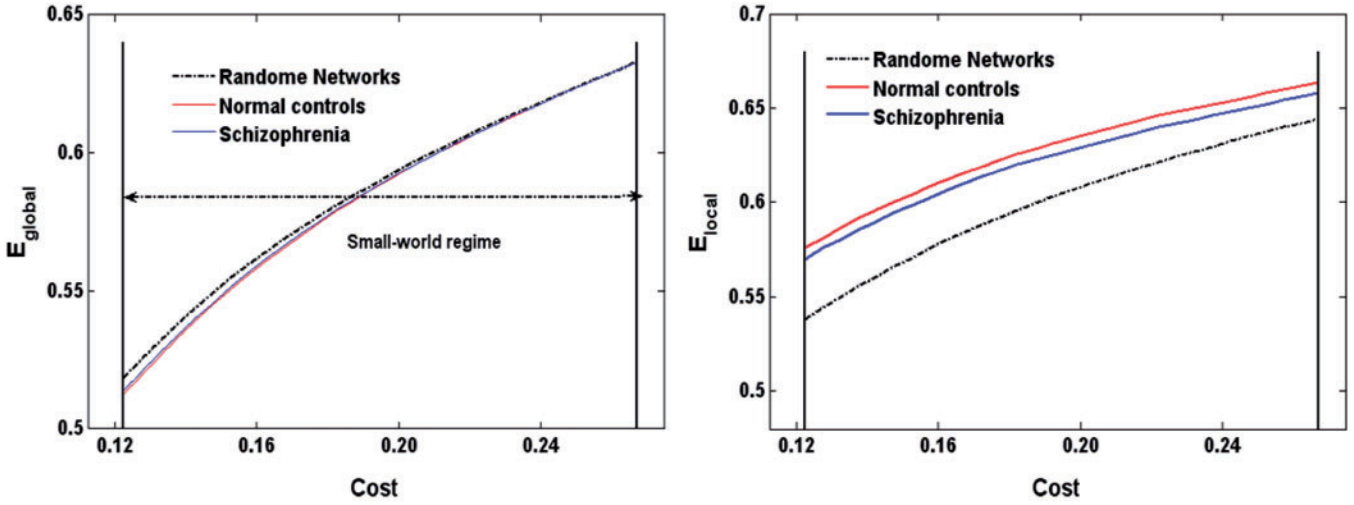

Fig. 2 Economic small-world human brain functional networks. (**A**) Global and (**B**) local efficiency for a random graph and brain networks as a function of cost. On average, over all subjects in each group, normal (blue line) and schizophrenia (red line) brain networks have lower efficiency than the limiting cases of random networks (black dashed line). The small-world regime is conservatively defined as the range of costs $0.122 \leqslant K_{cost} \leqslant 0.267$ for which the global efficiency curve for the normal networks is less than the global efficiency curve for the random networks.

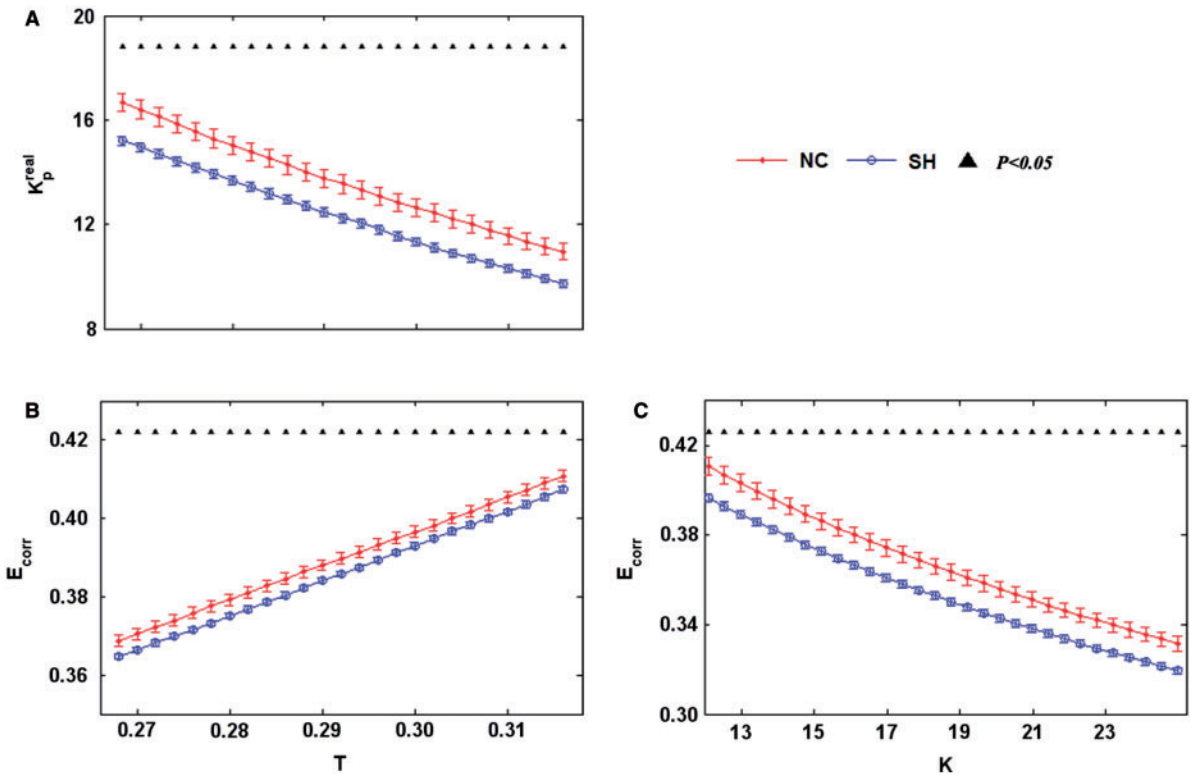

Fig. 3 (**A**) Mean degree of connectivity, K_p^{real}, and (**B**) strength of functional connectivity, E_{corr}, for schizophrenic (blue squares) and healthy (red dots) subjects as a function of threshold *T*. (**C**) strength of functional connectivity, E_{corr}, for schizophrenic (blue squares) and healthy (red dots) subjects as a function of degree *K*. Error bars correspond to standard error of the mean. Black triangles indicate where the difference between the two groups is significant (*t*-test, $P < 0.05$).

subjects (Fig. 4B). When looking at the absolute clustering coefficients and the absolute path length as a function of *K*, we found the absolute clustering coefficient increased and the shortest absolute path length decreased with an increase in the degree *K*, and only the absolute clustering coefficient showed a significant difference between the two groups (Fig. 4C).

The small-world attribute is evident in the brain networks of both groups: γ is significantly greater than 1 while λ is near

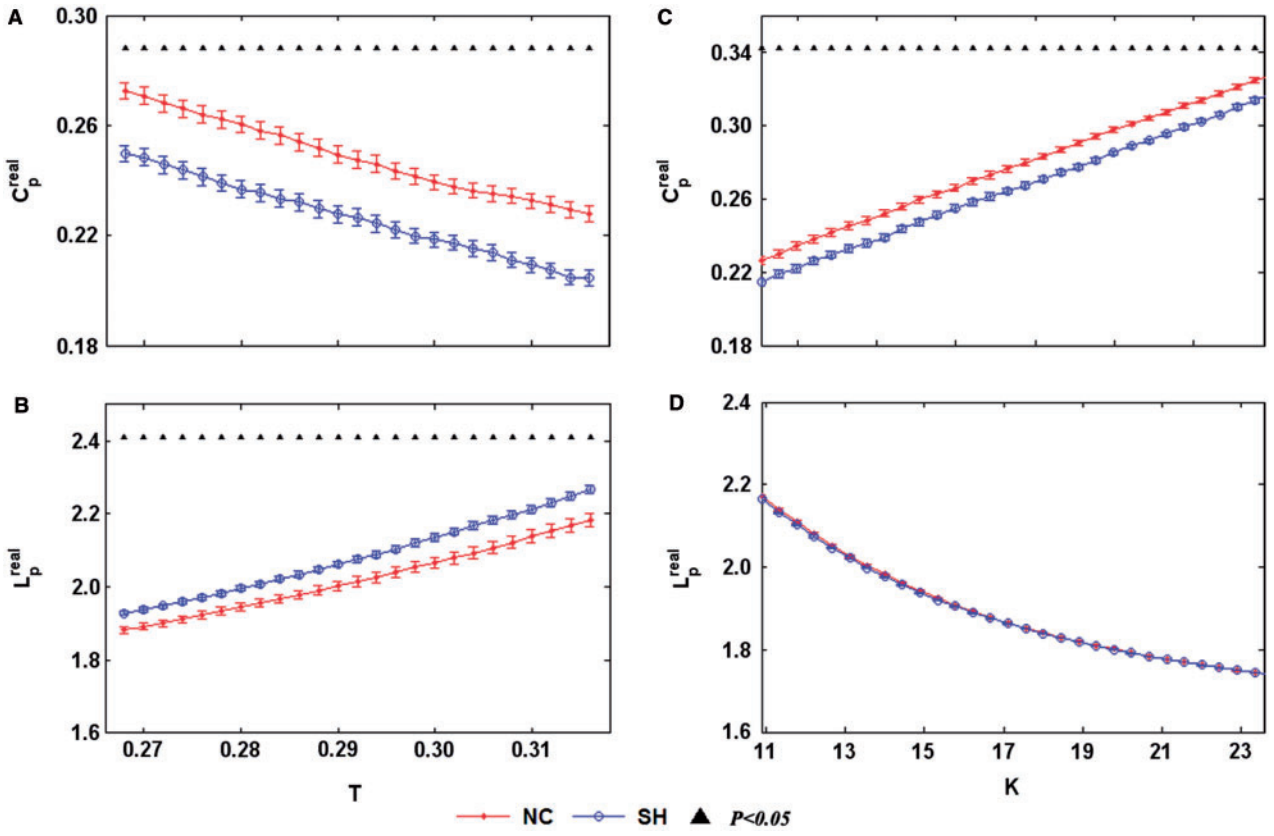

Fig. 4 (**A**) Mean absolute clustering coefficient, C_p^{real}, and (**B**) absolute path length, L_p^{real}, for schizophrenic (blue squares) and healthy (red dots) subjects as a function for *T*. (**C**) Mean absolute clustering coefficient, C_p^{real}, and (**D**) absolute path length, L_p^{real}, for schizophrenic (blue squares) and healthy (red dots) subjects as a function of *K*. Error bars correspond to standard error of the mean. Black triangles indicate where the difference between the two groups is significant (*t*-test, $P < 0.05$).

the value of 1 over the whole range of *T* or *K*. Due to the large variance, there were no statistically significant differences in the values of γ, λ or σ between the two groups when the same threshold was used (Fig. 5A–C). γ and σ were significantly decreased in the patients with schizophrenia when using the same *K* for both groups (Fig. 5D and F). Only at a small number of connectivity values was λ found to show statistically significant differences between the two groups (Fig. 5E). The fact that we found significant differences between the two groups indicates that small-world properties are disrupted in patients with schizophrenia.

Global efficiency is a measure of the transfer speed of parallel information in the brain; whereas local efficiency is a measure of the information exchange of each subgraph (Achard and Bullmore, 2007). Global efficiency of brain functional networks were compared with the parameters estimated in a random graph with the same degree distribution over a range of network costs. As expected, efficiency monotonically increased as a function of cost in all networks; the random graph had higher global efficiency and lower local efficiency than the healthy subjects' (Fig. 2A and B) which is consistent with the previous study (Achard and Bullmore, 2007). The global and local efficiencies of the brain functional networks in the patients with schizophrenia were disrupted as a function of threshold (Fig. 6A and B). And the local efficiencies of the brain functional networks in the patients with schizophrenia were disrupted as a function of degree of connectivity (Fig. 6D). However, there was no significant difference in global and local efficiency between the two groups (Fig. 6C).

Distribution of the altered regions in the brain

We used a two-sample two-tailed *t*-test to detect statistical differences in the small-world topological properties between schizophrenic patients and the healthy subjects for each brain region at each selected threshold (or degree of connectivity). We found the pattern of small-world topological properties to be significantly altered in many brain regions in the prefrontal, parietal and temporal lobes (Figs. S7 and S8). Since all thresholds were similar in their trends with respect to the differences in their small-world properties between the schizophrenic patients and the healthy subjects, we have chosen to report only one typical threshold ($T = 0.316$, the top of the threshold range) (Fig. 7) and degree of connectivity ($K = 10.9$, the smallest degree in this study) (Fig. 8) in the main text. Details can be found in part III of the Supplementary Material.

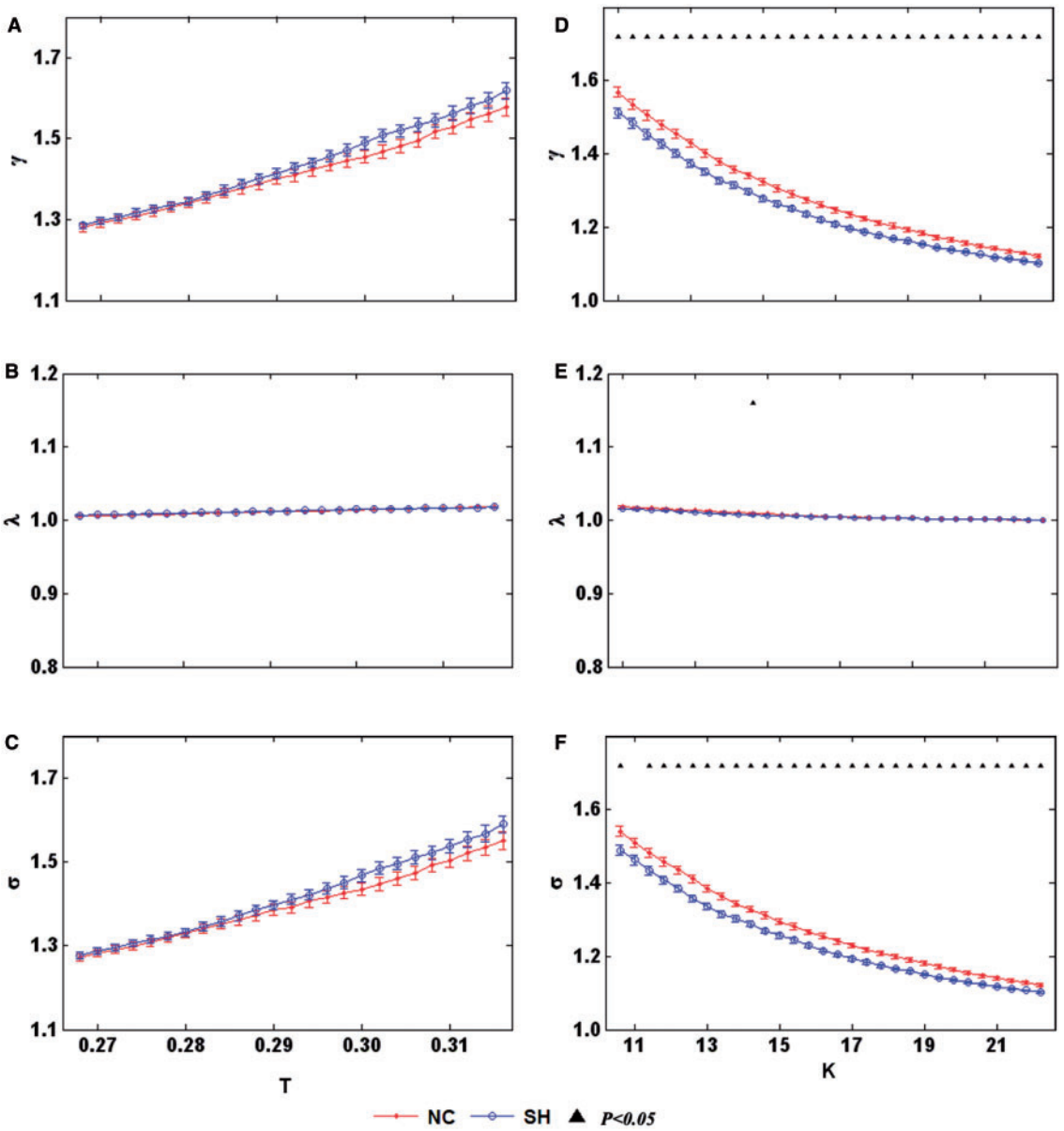

Fig. 5 (**A**) γ, (**B**) λ and (**C**) σ for schizophrenic (blue squares) and healthy (red dots) subjects as a function of threshold. (**D**) γ, (**E**) λ and (**F**) σ for schizophrenic (blue squares) and healthy (red dots) subjects as a function of K. Error bars correspond to standard error of the mean. Black triangles indicate where the difference between the two groups is significant (t-test, $P < 0.05$).

Relationship between the altered topological measurements and the clinical variables

We found that the degree of connectivity, E_{corr}, K_p, C_p^{real}, E_{global} and E_{local} were negatively correlated; however, L_p^{real} was positively correlated with illness duration when these measurements were computed as a function of each threshold (Fig. S9). We show this pattern at a typical threshold $T = 0.316$ in Fig. 9. A similar pattern was found when the relationship between these topological measurements and the clinical variables was investigated as a function of the degrees of connectivity (Figs. 10 and S10). (For further detail, please see Figs. S9 and S10 of part IV in the Supplementary Material.)

Discussion

In the present study, resting-state fMRI data were used to construct functional brain networks in schizophrenic and healthy subjects. We thresholded the partial correlation matrices to construct a set of undirected binary graphs for each subject and compared the topological properties of brain functional networks between the two groups. The brain functional networks of the healthy subjects showed efficient small-world structure, which is consistent with several previous studies (Stam, 2004; Achard *et al.*, 2006; Bassett and Bullmore, 2006; Bassett *et al.*, 2006; Achard and Bullmore, 2007). Nevertheless, the patients with

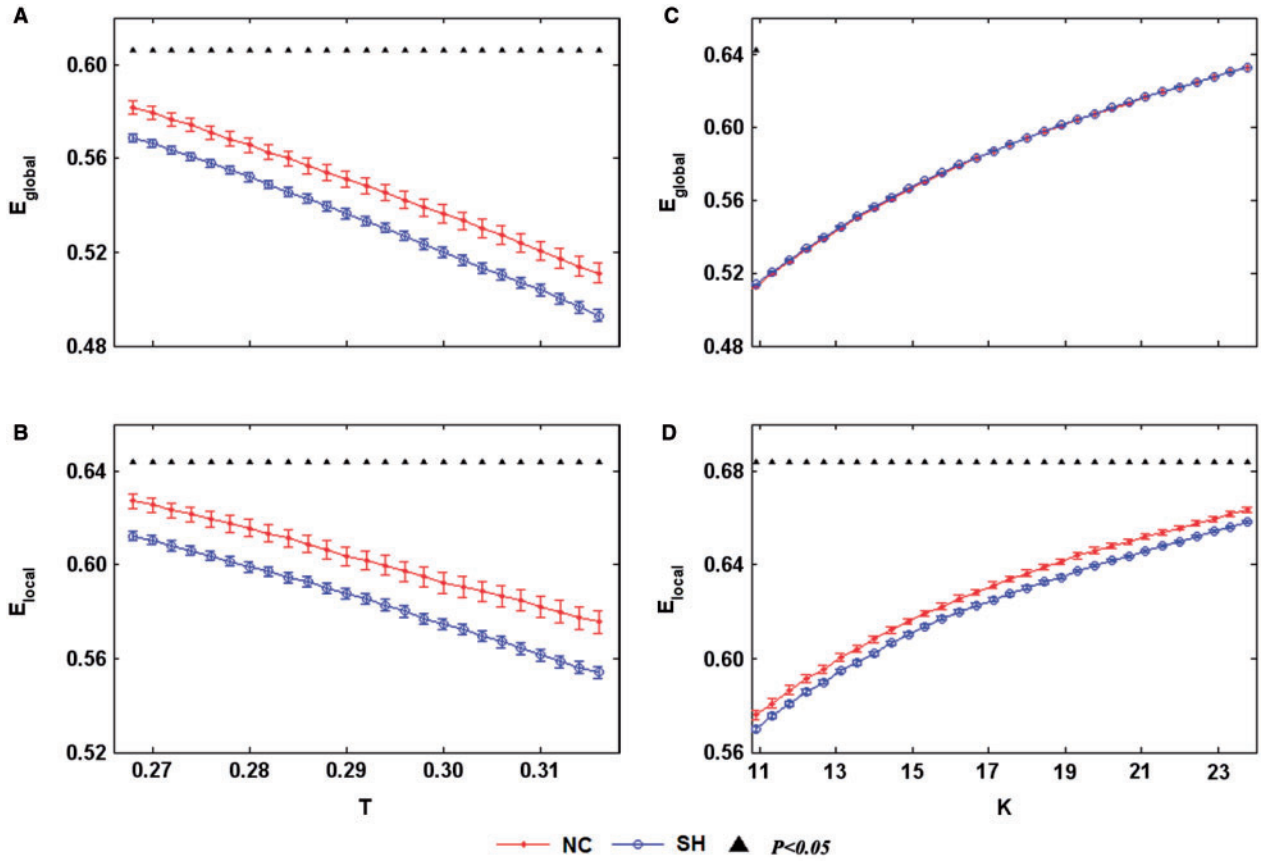

Fig. 6 (**A**) Mean global efficiency, E_{global}, and (**B**) local efficiency, E_{local}, for schizophrenic (blue squares) and healthy (red dots) subjects as a function of *T*. (**C**) Mean global efficiency, E_{global}, and (**D**) local efficiency, E_{local}, for schizophrenic (blue squares) and healthy (red dots) subjects as a function of degree. Error bars correspond to standard error of the mean. Black triangles indicate where the difference between the two groups is significant (*t*-test, $P < 0.05$).

schizophrenia showed disturbed topological properties, such as a lower degree of connectivity, a lower strength of connectivity, a lower absolute clustering coefficient, and a longer absolute path length compared with those of healthy subjects. All these findings support the hypothesis that schizophrenia is a disorder of dysfunctional integration among large, distant brain regions (Bullmore *et al.*, 1997, 1998; Friston, 2005). These results are consistent with a previous EEG study, in which disrupted small-world properties were found in the alpha, beta and gamma bands during resting-state and working memory tasks in patients with schizophrenia (Micheloyannis *et al.*, 2006*a*). More importantly, we found that the topological measurements of efficient small-world brain functional networks were correlated with illness duration in schizophrenia.

Disrupted efficient small-world properties in schizophrenia

Efficient small-world brain network

The human brain is a large, dynamic functional network with an economical, small-world architecture and is characterized by high local clustering of connections between neighbouring nodes but with short path lengths between any pair of nodes (Sporns and Honey, 2006; Achard and Bullmore, 2007). Functional segregation and integration are two major organizational principles of the human brain. In other words, an optimal brain requires a suitable balance between local specialization and global integration of brain functional activity (Tononi *et al.*, 1998). This is supported by higher absolute clustering coefficients (an index of functional segregation) and shorter absolute path length (an index of functional integration) in the functional brain networks of healthy subjects.

The small-world attributes reflect the need of the functional brain network to satisfy the opposing demands of local and global processing (Kaiser and Hilgetag, 2006). This issue is supported by many previous studies based on MEG (Stam, 2004), EEG (Micheloyannis *et al.*, 2006*b*) and fMRI (Eguiluz *et al.*, 2005; Salvador *et al.*, 2005*a*; Achard *et al.*, 2006). In the present study, we found that the resting brain functional network of the healthy subjects had salient small-world properties (Figs 5 and 6). Our results are in line with those of several previous brain network studies (Hilgetag *et al.*, 2000; Stam, 2004; Salvador *et al.*, 2005*a*; Achard *et al.*, 2006; Micheloyannis *et al.*, 2006*a*; Stam *et al.*, 2007) (Table 4).

Table 4 Small-world properties of brain networks shown in the present study and previous studies

		γ	λ
Present study[a]	Healthy subjects	1.57	1.02
	Schizophrenia patients	1.51	1.02
Hilgetag *et al.* (2000)	Healthy subjects	1.58	1.07
	Cat whole cortex	1.99	1.07
Stam (2004)[b]	Healthy subjects	1.89	1.19
Salvador *et al.* (2005*a*)	Healthy subjects	2.08	1.09
Archard *et al.* (2006)[c]	Healthy subjects	2.38	1.08
Stam *et al.* (2007)[d]	AD patients	1.6	1.12
	Healthy subjects	1.58	1.07
Micheloyannis *et al.* (2006*a*)[e]	Healthy subjects	1.95	1.19
	Schizophrenia patients	1.82	1.13

[a]Data are shown for the same $K = 10.9$ ($N = 90$).
[b]Data are shown for the gamma band of EEG signals and $K = 20$.
[c]The mean cluster coefficients and the minimum path length were computed from the 0.03–0.06 Hz resting state fMRI signals.
[d]Data are shown for the beta band of EEG signals and $N = 21$, $K = 3$.
[e]Data are shown for the theta band of EEG signals in a working memory task at $K = 5$ ($N = 28$).

Disrupted efficient small-world characters in schizophrenia

More importantly, over a wide range of thresholds and the degree of connectivity, K, the absolute clustering coefficients, C_p^{real}, showed significantly smaller values in schizophrenia, implying relatively sparse local connectedness of the brain functional networks in schizophrenia (Micheloyannis *et al.*, 2006*a*). In addition, the strength of functional connectivity showed significantly lower values in patients with schizophrenia. This means that the extent of local connectedness decreased in the schizophrenia group. Information interactions between interconnected brain regions are believed to be a basis of human cognitive processes (Pastor *et al.*, 2000; Horwitz, 2003; Stam *et al.*, 2007). Short absolute path lengths have been demonstrated to promote effective interactions between and across different cortical regions (Bassett and Bullmore, 2006; Achard and Bullmore, 2007). The longer absolute path lengths may indicate that information interactions between interconnected brain regions are slower and less efficient in schizophrenia. Thus, the lower degree of

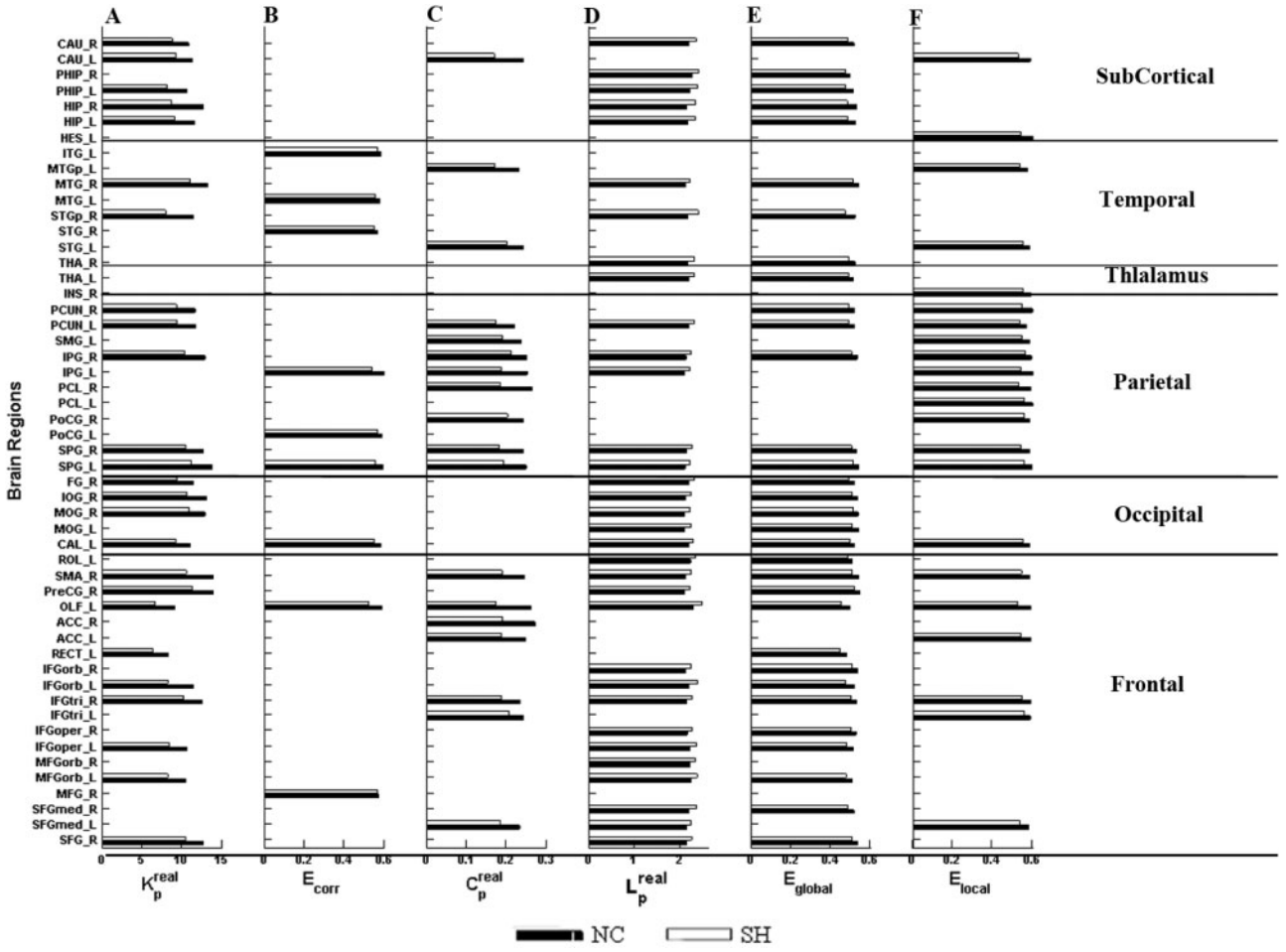

Fig. 7 Distribution of brain regions in which small-world properties [(**A**) K_p^{real}, (**B**) E_{corr}, (**C**) C_p^{real}, (**D**) L_p^{real}, (**E**) E_{global} and (**F**) E_{local}] altered significantly in healthy subjects (black) and schizophrenia patients (white) at a selected threshold T ($T = 0.316$). Bars indicate that the area shows significant altered in the relative measurement, and the length of the bar indicates the mean value of the relative measurement between the two groups.

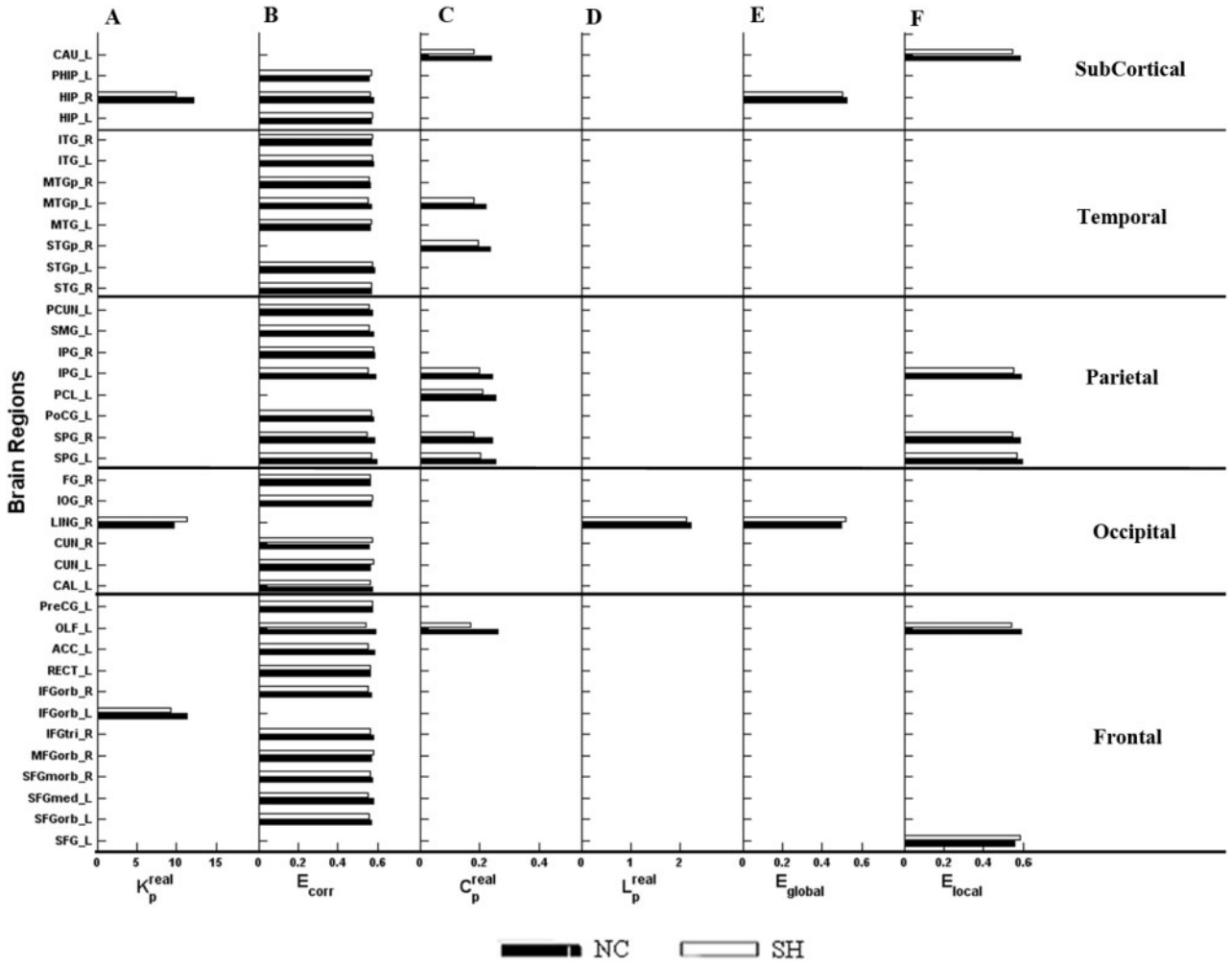

Fig. 8 Distribution of brain regions in which small-world properties [(**A**) K_p^{real}, (**B**) E_{corr}, (**C**) C_p^{real}, (**D**) L_p^{real}, (**E**) E_{global} and (**F**) E_{local}] altered significantly in healthy subjects (black) and schizophrenia patients (white) at a selected degree of connectivity K ($K = 10.9$). Bars indicate that the area shows significant altered in the relative measurement, and the length of the bar indicates the mean value of the relative measurement between the two groups.

connectivity, the lesser strength of connectivity, the lower absolute clustering coefficients and the longer absolute path length as a function of T or K indicate a dysfunctional organization of the brain functional network in schizophrenia.

We found that the γ values did not show significant differences between groups when the same thresholds were applied to both groups, and at some thresholds the γ even showed lower values in healthy subjects, which may be due to the higher degree of the corresponding random networks for healthy subjects (Stam *et al.*, 2007). To control this effect, we compared the γ values between the two groups as a function of K, i.e. each subject has the same number of edges for both groups. The results showed that schizophrenia patients had a significantly lower γ's compared with healthy subjects at the same degree. Our findings are consistent with the previous findings of the presence of a small-world brain functional network in healthy subjects; however, these topological structures of the brain functional network are disrupted in schizophrenia (Liang *et al.*, 2006*b*; Micheloyannis *et al.*, 2006*a*).

Our results (Figs 3 and 4) are in line with a previous EEG study in which schizophrenic patients showed smaller absolute clustering coefficients but relatively longer absolute path lengths during the resting-state. Moreover, it should be noted that the reduction of the absolute clustering coefficient for schizophrenia patients in the earlier EEG study is larger than in our study (Micheloyannis *et al.*, 2006*a*). The most likely explanation for this difference is a longer duration of the illness of the patients in the study by Micheloyannis *et al.* (2006*a*). The mean illness duration was 120 months in that study; whereas the mean illness duration of our patients was 27 months (Table 1). This was also consistent with our finding that there was a significant correlation between the absolute clustering coefficient and the duration of the illness; a longer duration of the illness induced a smaller absolute clustering coefficient (Figs 7 and 8). Another possible reason is that differences in data acquisition techniques or network size could cause changes in the topological properties of the network.

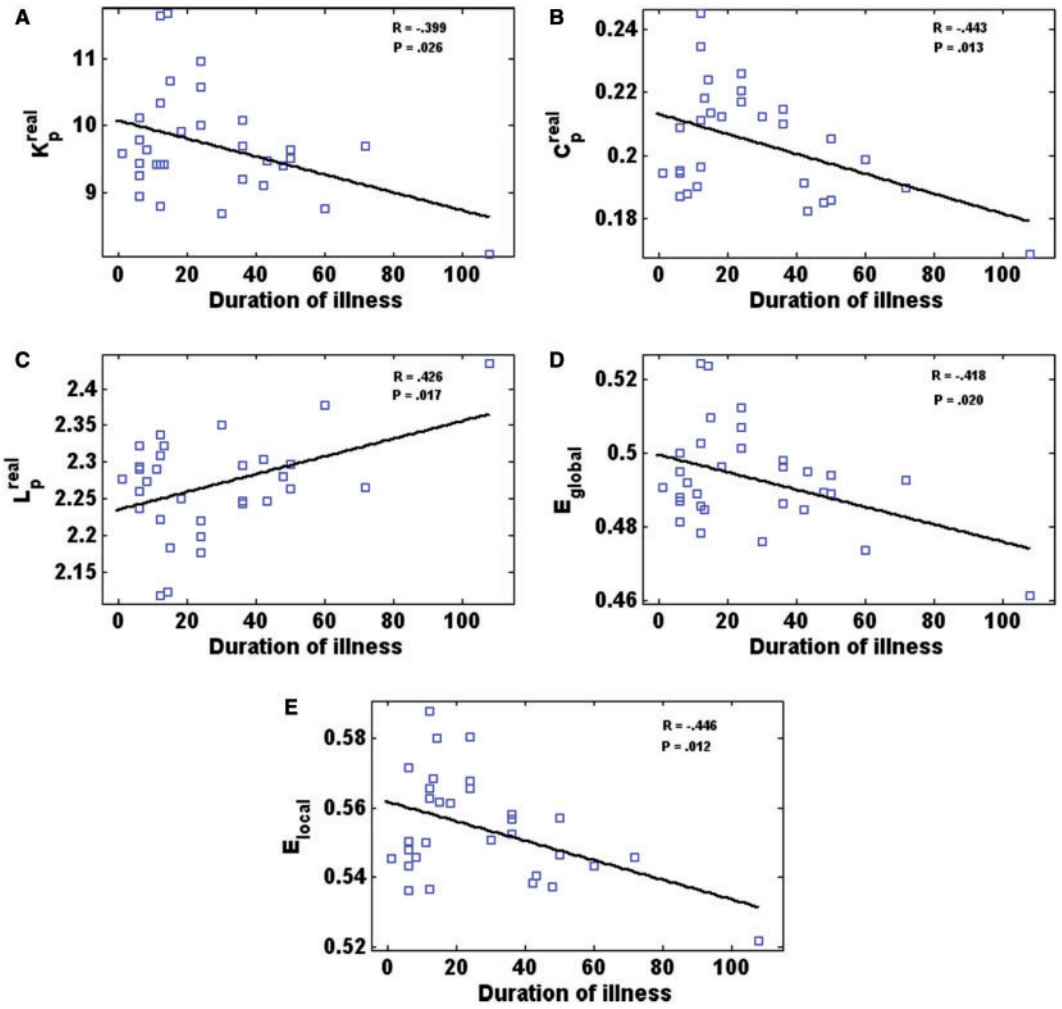

Fig. 9 Scatter plots with trend line showing the topological properties (K_p^{real}, C_p^{real}, L_p^{real}, E_{global}, E_{local}) of the brain functional networks (open blue squares) as a function of illness duration for a selected T ($T = 0.316$) in patients with schizophrenia. Pearson correlation coefficient for K_p^{real} ($R = -0.399$, $P = 0.026$) (**A**), C_p^{real} ($R = -0.443$, $P = 0.013$) (**B**), L_p^{real} ($R = 0.426$, $P = 0.017$) (**C**), E_{global} ($R = -0.418$, $P = 0.020$) (**D**) and E_{local} ($R = -0.446$, $P = 0.012$) (**E**) were significant.

Networks with small-world attributes confer resilience against pathological attack and support parallel, segregated and distributed information processing at a relatively high efficiency (Achard and Bullmore, 2007). The efficiency measure provides us with a precise quantitative analysis of the information transfer among brain regions; it also indicates that in the neural cortex each region is intermingled with others allowing a perfect balance between local necessities and a wide scope of interactions (Latora and Marchiori, 2001). Our results not only demonstrate that interregional relationships in brain activity are indeed disrupted in schizophrenia, but also show for the first time that patients with schizophrenia have lower efficiency in parallel information transfer in the brain network (Fig. 6). This is consistent with the increasing evidence that schizophrenia can be considered as a disorder of dysfunctional integration among different brain regions.

In the current study, we found that in many brain regions in the frontal, parietal and temporal lobes the small-world properties were significantly altered (Figs 7 and 8 and Figs. S7 and S8). For example, we found that the degree of connectivity is smaller in many brain areas in the frontal lobe in the patient group (Fig. 7), which indicates a lower connectivity between the regions in this lobe with other brain regions. This might lead to longer absolute path lengths in many regions of the frontal lobes in patients with schizophrenia. This is consistent with many previous studies in which the functional connectivity of the frontal (Fletcher *et al.*, 1999*a*; Meyer-Lindenberg *et al.*, 2001; Tan *et al.*, 2006), parietal (Danckert *et al.*, 2004) and temporal lobes (Fletcher *et al.*, 1999*b*; Garrity *et al.*, 2007) were disturbed in this disorder.

Relationship between topological measurements and duration of illness

Importantly, we found that the topological measurements of the small-world brain functional networks were correlated with illness duration. A longer duration of the illness induced

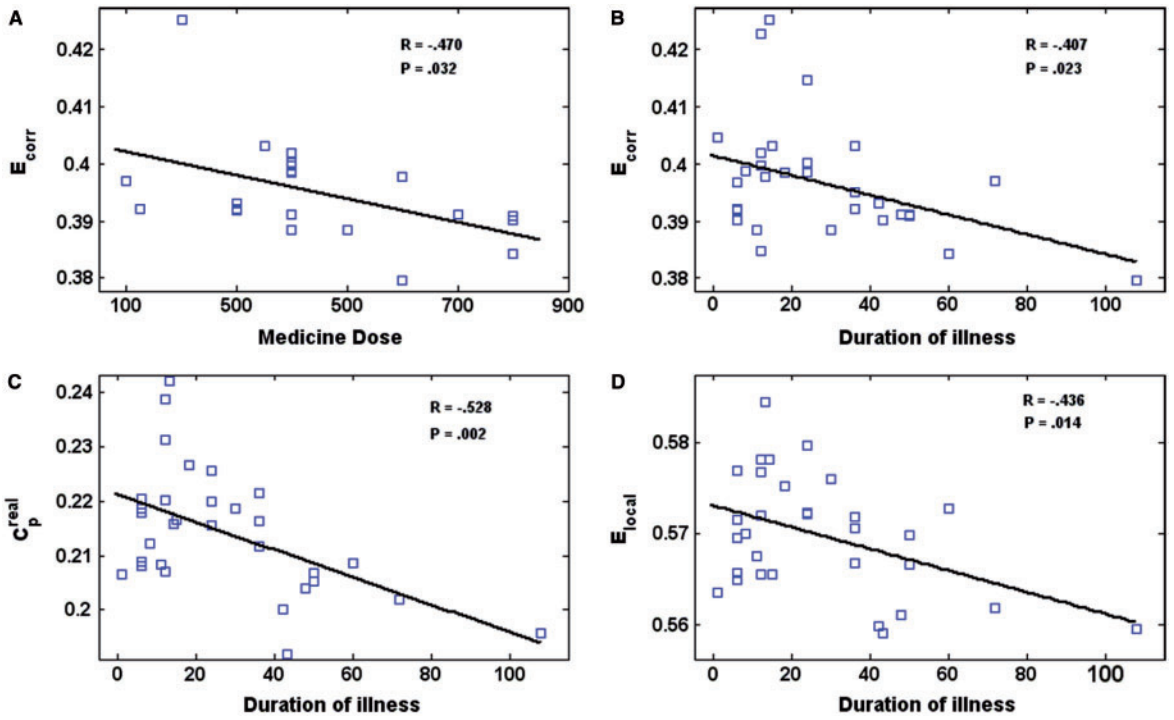

Fig. 10 Scatter plots with trend line showing the topological properties (E_{corr}, C_p^{real}, E_{local}) of the brain functional networks (open blue squares) as a function of illness duration for a selected K in patients with schizophrenia. Pearson correlation coefficient between E_{corr} and medication dosed ($R = -0.470$, $P = 0.032$) (**A**) were significant in the medication patients. Pearson correlation coefficient for E_{corr} ($R = -0.407$, $P = 0.023$) (**B**), and C_p^{real} ($R = -0.528$, $P = 0.002$) (**C**) and E_{local} ($R = -0.436$, $P = 0.014$) (**D**) were significant.

a smaller absolute clustering coefficient, a lower degree of connectivity, a lower global and local efficiency, and a longer absolute path length of brain functional networks (Figs 9 and 10 and Figs S9 and S10). These findings appear to demonstrate that the severity of the disruption of the efficient small-world structure of the brain is related to the duration of the illness. In addition, the significant negative correlation between the strength of the functional connectivity and the chlorpromazine-equivalent medication dosage (Figs. 10A and S10) may indicate that in patients with schizophrenia the more severe the illness, the weaker the functional connectivity between the regions of the brain.

The findings in the present study provide further evidence for schizophrenia as a disconnection syndrome (Friston and Frith, 1995; Bullmore *et al.*, 1997; Friston, 2002, 2005). Detection and estimation of the small-world topological measurements could help us better understand the pathophysiological mechanism of schizophrenia.

Methodological considerations

Effect of morphometric changes on functional connectivity analysis

Changes in the volume of the frontal lobe, temporal lobe and their sub-regions over the course of illness have been well studied in patients with schizophrenia (Giedd *et al.*, 1999; Bachmann *et al.*, 2004; Molina *et al.*, 2004, 2006; Premkumar *et al.*, 2006). A recent meta-analysis indicated that the left superior temporal gyrus and the left medial temporal lobe are the key regions of structural alteration in patients with schizophrenia (Honea *et al.*, 2005). To assess whether the structural alterations have an influence on altered small-world properties in patients with schizophrenia, we analysed our data for structural differences between the two groups. We divided the grey matter of the entire brain according to an anatomically labelled template, and then investigated the difference at each brain region. There were no significant differences found in brain regions between the two groups ($P < 0.05$, FDR corrected). Although other studies have reported such differences (Giedd *et al.*, 1999; Bachmann *et al.*, 2004; Molina *et al.*, 2004, 2006; Premkumar *et al.*, 2006), our failure to detect them does not mean that they do not exist. Our analyses and methodologies may have disguised such changes. For example, our use of an anatomically labelled template may have caused atrophied areas to be separated into different, but adjacent, brain regions, making them difficult to detect. To further reduce the effects of grey matter atrophy on our results, we regressed out the confounding factor of grey matter atrophy, and then constructed a set of functional brain networks using a wide range of thresholds (or degrees of connectivity). The results obtained after eliminating the possible influence of grey matter atrophy were similar to those obtained without eliminating this influence. Extended details can be found in the part V of the supplemental material.

Low-frequency fluctuations of resting-state fMRI

Low frequency (<0.1 Hz) fluctuations of resting-state fMRI signals have been strongly suggested to be neurobiologically interesting and related to spontaneous neural activity (Biswal *et al.*, 1995) and endogenous/background neurophysiologic process of the human brain (Raichle and Gusnard, 2005; Raichle and Mintun, 2006). Furthermore, resting-state fMRI has practical advantages for clinical applications because no stimulation and response are required, thus it can be performed easily by subjects, especially patients. Because of this, although resting-state fMRI is a relatively young technique, many exciting findings have been reported in the past several years. Functional correlation may reflect endogenously coordinated, dynamic activity in large-scale neuronal populations in healthy subjects. In addition, the altered patterns of functional connectivity based on resting-state fMRI have been suggested to be pathophysiologically meaningful in some diseases (Fox and Raichle, 2007). For these reasons, we believe that it is significant to investigate the topological properties of the brain functional network of patients with schizophrenia based on resting-state fMRI data.

Effect of the length of the time series

It should also be noted that we used relatively shorter time series (170 volumes per subject) compared to several previous resting-state fMRI studies (e.g. 2048 volumes in Bullmore and colleagues' previous studies) (Salvador *et al.*, 2005*a*; Achard *et al.*, 2006). However, our results on healthy subjects are compatible with these previous studies (extended details can be found in the part VI in the supplemental material). In addition, we compared many earlier resting-state fMRI studies that used either short or long time series (80–2048 volumes of resting-state fMRI signals) and found that they produced replicable results in normal people (Greicius *et al.*, 2003; Fox *et al.*, 2005; Salvador *et al.*, 2005*a*; Achard and Bullmore, 2007) and in some cognitive disorders, such as in Alzheimer's disease (Greicius *et al.*, 2004; Sorg *et al.*, 2007; Wang *et al.*, 2007), major depression (Greicius *et al.*, 2007) and schizophrenia (Liang *et al.*, 2006b; Zhou *et al.*, 2007*a*, *b*). Consequently, this suggests that a relatively small number of volumes may be sufficient to get enough information during rest. Nonetheless, determining the appropriate number of volumes remains an interesting topic for future resting-state fMRI studies.

Some limitations

It should be noted that there are some additional limitations in methodology and materials in the present study. Like most functional connectivity studies based on resting-state fMRI, we cannot eliminate the effects of physiologic noise because we used a relatively low sampling rate (TR = 2 s) for multi-slice acquisitions. Under this sampling rate, respiratory and cardiac fluctuations may be present in the fMRI time series; although a band-pass filtering of 0.01∼0.08 Hz was used to reduce physiological noise. These respiratory and cardiac fluctuations may reduce the specificity of low frequency fluctuations to functional connected regions (Lowe *et al.*, 1998).

Another limitation is that, from the perspective of materials, we cannot eliminate the effects of heterogeneity with respect to clinical symptoms, duration of illness, severity of symptoms and medication among the patients. Many of these factors, such as clinical symptoms (Strous *et al.*, 2004; Hazlett *et al.*, 2007), duration of non-treatment (Perkins *et al.*, 2005) and medication (Strous *et al.*, 2004; Davis *et al.*, 2005; Lieberman *et al.*, 2005), have been shown to be related to brain functioning in patients. A large sample of first episode schizophrenic patients is needed in future research to support the findings of the present study.

Conclusion

Our results support the concept that the brain functional network is a large complex of networks with optimal economical small-world topological properties. Specifically, the present study shows that the spatial topological pattern of the brain functional network is altered in the frontal, parietal and temporal lobes in patients with schizophrenia, which lends itself to an interpretation of disorganization of neural networks in this illness. The smaller degree of connectivity and the lower strength of the functional connectivity not only demonstrate the sparse connectedness but also indicate a decreased synchronization of functionally related brain regions in schizophrenia. A longer absolute path length with a smaller absolute clustering coefficient suggests a loss of complexity and a less than optimal organization of the brain functional network. This disruption may partially account for the reduced global/local efficiency of information processing within the brain, which may lead to the deficits of cognition and behaviour of patients with schizophrenia. The current study has identified deficits in the spatial organization of the human brain functional network in patients with schizophrenia. These findings are comparable with contemporary dysfunctional integration theories regarding the pathophysiological basis of schizophrenia. The correlation between the topological measures of the efficient small-world attributes and illness duration in schizophrenia leads us to believe that this method could be helpful for understanding the dysfunction syndrome in schizophrenia. This approach may also be able to be used in other disorders such as Alzheimer's disease, which can also be taken as a disconnection syndrome and in which abnormal functional connectivity plays a role.

Supplementary material

Supplementary material is available at *Brain* online.

Acknowledgements

The authors are grateful to Prof. Edward Bullmore, Kun Wang and Lijuan Xu for their constructive comments and

suggestions. The authors are grateful to the anonymous referees for their significant and constructive comments and suggestions, which greatly improved the paper. The authors express appreciation to Drs Rhoda E. and Edmund F. Perozzi for English language and editing assistance. The authors also thank Fan Kuang for helping in collecting samples. This work was partially supported by the Natural Science Foundation of China, Grant Nos. 30425004, 30530290 and 30670752, and the National Key Basic Research and Development Program (973), Grant No. 2004CB318107.

References

Achard S, Bullmore E. Efficiency and cost of economical brain functional networks. PLoS Comput Biol 2007; 3: e17.

Achard S, Salvador R, Whitcher B, Suckling J, Bullmore E. A resilient, low-frequency, small-world human brain functional network with highly connected association cortical hubs. J Neurosci 2006; 26: 63–72.

Andreasen NC, Paradiso S, O'Leary DS. "Cognitive dysmetria" as an integrative theory of schizophrenia: a dysfunction in cortical-subcortical-cerebellar circuitry? Schizophr Bull 1998; 24: 203–18.

Bachmann S, Bottmer C, Pantel J, Schroder J, Amann M, Essig M, et al. MRI-morphometric changes in first-episode schizophrenic patients at 14 months follow-up. Schizophr Res 2004; 67: 301–3.

Bassett DS, Bullmore E. Small-world brain networks. Neuroscientist 2006; 12: 512–23.

Bassett DS, Meyer-Lindenberg A, Achard S, Duke T, Bullmore E. Adaptive reconfiguration of fractal small-world human brain functional networks. Proc Natl Acad Sci USA 2006; 103: 19518–23.

Biswal B, Yetkin FZ, Haughton VM, Hyde JS. Functional connectivity in the motor cortex of resting human brain using echo-planar MRI. Magn Reson Med 1995; 34: 537–41.

Bluhm RL, Miller J, Lanius RA, Osuch EA, Boksman K, Neufeld RW, et al. Spontaneous low-frequency fluctuations in the BOLD signal in schizophrenic patients: anomalies in the default network. Schizophr Bull 2007; 33: 1004–12.

Bullmore ET, Frangou S, Murray RM. The dysplastic net hypothesis: an integration of developmental and dysconnectivity theories of schizophrenia. Schizophr Res 1997; 28: 143–56.

Bullmore ET, Woodruff PW, Wright IC, Rabe-Hesketh S, Howard RJ, Shuriquie N, et al. Does dysplasia cause anatomical dysconnectivity in schizophrenia? Schizophr Res 1998; 30: 127–35.

Danckert J, Saoud M, Maruff P. Attention, motor control and motor imagery in schizophrenia: implications for the role of the parietal cortex. Schizophr Res 2004; 70: 241–61.

Davis CE, Jeste DV, Eyler LT. Review of longitudinal functional neuroimaging studies of drug treatments in patients with schizophrenia. Schizophr Res 2005; 78: 45–60.

Eguiluz VM, Chialvo DR, Cecchi GA, Baliki M, Apkarian AV. Scale-free brain functional networks. Phys Rev Lett 2005; 94: 018102.

First M, Spitzer R, Gibbon M, Williams J. Structured clinical interview for DSM-IV Axis I Disorder-Patient Edition (SCID-I/P,Version 2.0), Biometrics Research Department, New York State Psychiatric Institute. New York; 1995.

Fletcher P, Buchel C, Josephs O, Friston K, Dolan R. Learning-related neuronal responses in prefrontal cortex studied with functional neuroimaging. Cereb Cortex 1999a; 9: 168–78.

Fletcher P, McKenna PJ, Friston KJ, Frith CD, Dolan RJ. Abnormal cingulate modulation of fronto-temporal connectivity in schizophrenia. Neuroimage 1999b; 9: 337–42.

Fox MD, Raichle ME. Spontaneous fluctuations in brain activity observed with functional magnetic resonance imaging. Nat Rev Neurosci 2007; 8: 700–11.

Fox MD, Snyder AZ, Vincent JL, Corbetta M, Van Essen DC, Raichle ME. The human brain is intrinsically organized into dynamic, anticorrelated functional networks. Proc Natl Acad Sci USA 2005; 102: 9673–8.

Friston KJ. Dysfunctional connectivity in schizophrenia. World Psychiatry 2002; 1: 66–71.

Friston KJ. Disconnection and cognitive dysmetria in schizophrenia. Am J Psychiatry 2005; 162: 429–32.

Friston KJ, Frith CD. Schizophrenia: a disconnection syndrome? Clin Neurosci 1995; 3: 89–97.

Friston KJ, Frith CD, Liddle PF, Frackowiak RS. Functional connectivity: the principal-component analysis of large (PET) data sets. J Cereb Blood Flow Metab 1993; 13: 5–14.

Garrity AG, Pearlson GD, McKiernan K, Lloyd D, Kiehl KA, Calhoun VD. Aberrant "default mode" functional connectivity in schizophrenia. Am J Psychiatry 2007; 164: 450–7.

Giedd JN, Jeffries NO, Blumenthal J, Castellanos FX, Vaituzis AC, Fernandez T, et al. Childhood-onset schizophrenia: progressive brain changes during adolescence. Biol Psychiatry 1999; 46: 892–8.

Greicius MD, Flores BH, Menon V, Glover GH, Solvason HB, Kenna H, et al. Resting-state functional connectivity in major depression: abnormally increased contributions from subgenual cingulate cortex and thalamus. Biol Psychiatry 2007; 62: 429–37.

Greicius MD, Krasnow B, Reiss AL, Menon V. Functional connectivity in the resting brain: a network analysis of the default mode hypothesis. Proc Natl Acad Sci USA 2003; 100: 253–8.

Greicius MD, Srivastava G, Reiss AL, Menon V. Default-mode network activity distinguishes Alzheimer's disease from healthy aging: evidence from functional MRI. Proc Natl Acad Sci USA 2004; 101: 4637–42.

Hampson M, Peterson BS, Skudlarski P, Gatenby JC, Gore JC. Detection of functional connectivity using temporal correlations in MR images. Hum Brain Mapp 2002; 15: 247–62.

Hazlett EA, Romero MJ, Haznedar MM, New AS, Goldstein KE, Newmark RE, et al. Deficient attentional modulation of startle eyeblink is associated with symptom severity in the schizophrenia spectrum. Schizophr Res 2007; 93: 288–95.

He Y, Chen ZJ, Evans AC. Small-world anatomical networks in the human brain revealed by cortical thickness from MRI. Cereb Cortex 2007; 17: 2407–19.

Hilgetag CC, Burns GA, O'Neill MA, Scannell JW, Young MP. Anatomical connectivity defines the organization of clusters of cortical areas in the macaque monkey and the cat. Philos Trans R Soc Lond B Biol Sci 2000; 355: 91–110.

Honea R, Crow TJ, Passingham D, Mackay CE. Regional deficits in brain volume in schizophrenia: a meta-analysis of voxel-based morphometry studies. Am J Psychiatry 2005; 162: 2233–45.

Honey GD, Pomarol-Clotet E, Corlett PR, Honey RA, McKenna PJ, Bullmore ET, et al. Functional dysconnectivity in schizophrenia associated with attentional modulation of motor function. Brain 2005; 128: 2597–611.

Horwitz B. The elusive concept of brain connectivity. Neuroimage 2003; 19: 466–70.

Humphries MD, Gurney K, Prescott TJ. The brainstem reticular formation is a small-world, not scale-free, network. Proc Biol Sci 2006; 273: 503–11.

Kaiser M, Hilgetag CC. Nonoptimal component placement, but short processing paths, due to long-distance projections in neural systems. PLoS Comput Biol 2006; 2: e95.

Kim JJ, Ho Seok J, Park HJ, Soo Lee D, Chul Lee M, Kwon JS. Functional disconnection of the semantic networks in schizophrenia. Neuroreport 2005; 16: 355–9.

Kim JJ, Kwon JS, Park HJ, Youn T, Kang DH, Kim MS, et al. Functional disconnection between the prefrontal and parietal cortices during working memory processing in schizophrenia: a[15(O)]H2O PET study. Am J Psychiatry 2003; 160: 919–23.

Latora V, Marchiori M. Economic small-world behavior in weighted networks. Eur Phys J B 2003; 32: 249–63.

Latora V, Marchiori M. Efficient behavior of small-world networks. Phys Rev Lett 2001; 87: 198701.

Liang M, Jiang T, Tian L, Liu B, Zhou Y, Liu H, et al. An information-theoretic based method for constructing the complex brain functional network with fMRI and the analysis of small world property. In: Frangi A and Delingette H, editors. MICCAI 2006 Workshop Proceedings, From Statistical Atlases to Personalized Models: Understanding Complex Diseases in Populations and Individuals. Copenhagen, Denmark; 2006a. p. 23–6.

Liang M, Zhou Y, Jiang T, Liu Z, Tian L, Liu H, et al. Widespread functional disconnectivity in schizophrenia with resting-state functional magnetic resonance imaging. Neuroreport 2006b; 17: 209–13.

Lieberman JA, Stroup TS, McEvoy JP, Swartz MS, Rosenheck RA, Perkins DO, et al. Effectiveness of antipsychotic drugs in patients with chronic schizophrenia. N Engl J Med 2005; 353: 1209–23.

Liu Y, Yu C, Liang M, Li J, Tian L, Zhou Y, et al. Whole brain functional connectivity in the early blind. Brain 2007; 130: 2085–96.

Lowe MJ, Mock BJ, Sorenson JA. Functional connectivity in single and multislice echoplanar imaging using resting-state fluctuations. Neuroimage 1998; 7: 119–32.

Maslov S, Sneppen K. Specificity and stability in topology of protein networks. Science 2002; 296: 910–3.

Meyer-Lindenberg A, Poline JB, Kohn PD, Holt JL, Egan MF, Weinberger DR, et al. Evidence for abnormal cortical functional connectivity during working memory in schizophrenia. Am J Psychiatry 2001; 158: 1809–17.

Micheloyannis S, Pachou E, Stam CJ, Breakspear M, Bitsios P, Vourkas M, et al. Small-world networks and disturbed functional connectivity in schizophrenia. Schizophr Res 2006a; 87: 60–6.

Micheloyannis S, Pachou E, Stam CJ, Vourkas M, Erimaki S, Tsirka V. Using graph theoretical analysis of multi channel EEG to evaluate the neural efficiency hypothesis. Neurosci Lett 2006b; 402: 273–7.

Milo R, Shen-Orr S, Itzkovitz S, Kashtan N, Chklovskii D, Alon U. Network motifs: simple building blocks of complex networks. Science 2002; 298: 824–7.

Molina V, Sanz J, Sarramea F, Benito C, Palomo T. Lower prefrontal gray matter volume in schizophrenia in chronic but not in first episode schizophrenia patients. Psychiatry Res 2004; 131: 45–56.

Molina V, Sanz J, Sarramea F, Luque R, Benito C, Palomo T. Dorsolateral prefrontal and superior temporal volume deficits in first-episode psychoses that evolve into schizophrenia. Eur Arch Psychiatry Clin Neurosci 2006; 256: 106–11.

Pastor J, Lafon M, Trave-Massuyes L, Demonet JF, Doyon B, Celsis P. Information processing in large-scale cerebral networks: the causal connectivity approach. Biol Cybern 2000; 82: 49–59.

Paulus MP, Hozack NE, Zauscher BE, Frank L, Brown GG, McDowell J, et al. Parietal dysfunction is associated with increased outcome-related decision-making in schizophrenia patients. Biol Psychiatry 2002; 51: 995–1004.

Perkins DO, Gu H, Boteva K, Lieberman JA. Relationship between duration of untreated psychosis and outcome in first-episode schizophrenia: a critical review and meta-analysis. Am J Psychiatry 2005; 162: 1785–804.

Premkumar P, Kumari V, Corr PJ, Sharma T. Frontal lobe volumes in schizophrenia: effects of stage and duration of illness. J Psychiatr Res 2006; 40: 627–37.

Raichle ME, Gusnard DA. Intrinsic brain activity sets the stage for expression of motivated behavior. J Comp Neurol 2005; 493: 167–76.

Raichle ME, Mintun MA. Brain work and brain imaging. Annu Rev Neurosci 2006; 29: 449–76.

Salvador R, Suckling J, Coleman MR, Pickard JD, Menon D, Bullmore E. Neurophysiological architecture of functional magnetic resonance images of human brain. Cereb Cortex 2005a; 15: 1332–42.

Salvador R, Suckling J, Schwarzbauer C, Bullmore E. Undirected graphs of frequency-dependent functional connectivity in whole brain networks. Philos Trans R Soc Lond B Biol Sci 2005b; 360: 937–46.

Sorg C, Riedl V, Muhlau M, Calhoun VD, Eichele T, Laer L, et al. Selective changes of resting-state networks in individuals at risk for Alzheimer's disease. Proc Natl Acad Sci USA 2007; 104: 18760–5.

Spence SA, Liddle PF, Stefan MD, Hellewell JS, Sharma T, Friston KJ, et al. Functional anatomy of verbal fluency in people with schizophrenia and those at genetic risk. Focal dysfunction and distributed disconnectivity reappraised. Br J Psychiatry 2000; 176: 52–60.

Sporns O, Honey CJ. Small worlds inside big brains. Proc Natl Acad Sci USA 2006; 103: 19219–20.

Sporns O, Zwi JD. The small world of the cerebral cortex. Neuroinformatics 2004; 2: 145–62.

Stam CJ. Functional connectivity patterns of human magnetoencephalographic recordings: a 'small-world' network? Neurosci Lett 2004; 355: 25–8.

Stam CJ, Jones BF, Nolte G, Breakspear M, Scheltens P. Small-world networks and functional connectivity in Alzheimer's disease. Cereb Cortex 2007; 17: 92–9.

Strogatz SH. Exploring complex networks. Nature 2001; 410: 268–76.

Strous RD, Alvir JM, Robinson D, Gal G, Sheitman B, Chakos M, et al. Premorbid functioning in schizophrenia: relation to baseline symptoms, treatment response, and medication side effects. Schizophr Bull 2004; 30: 265–78.

Tan HY, Sust S, Buckholtz JW, Mattay VS, Meyer-Lindenberg A, Egan MF, et al. Dysfunctional prefrontal regional specialization and compensation in schizophrenia. Am J Psychiatry 2006; 163: 1969–77.

Tononi G, Edelman GM, Sporns O. Complexity and coherency: integrating information in the brain. Trends Cogn Sci 1998; 2: 474–84.

Tzourio-Mazoyer N, Landeau B, Papathanassiou D, Crivello F, Etard O, Delcroix N, et al. Automated anatomical labeling of activations in SPM using a macroscopic anatomical parcellation of the MNI MRI single-subject brain. Neuroimage 2002; 15: 273–89.

Wang K, Liang M, Wang L, Tian L, Zhang X, Li K, et al. Altered functional connectivity in early Alzheimer's disease: a resting-state fMRI study. Hum Brain Mapp 2007; 28: 967–78.

Watts DJ, Strogatz SH. Collective dynamics of 'small-world' networks. Nature 1998; 393: 440–2.

Whittaker J. Graphical models in applied multivariate statistics. Chichester: Wiley; 1990.

Zhou Y, Liang M, Jiang T, Tian L, Liu Y, Liu Z, et al. Functional dysconnectivity of the dorsolateral prefrontal cortex in first-episode schizophrenia using resting-state fMRI. Neurosci Lett 2007a; 417: 297–302.

Zhou Y, Liang M, Tian L, Wang K, Hao Y, Liu H, et al. Functional disintegration in paranoid schizophrenia using resting-state fMRI. Schizophr Res 2007b; 97: 194–205.